Pretransitional orientational ordering of rigid-rod polymers in shear flow

Chaohua Wang, B. E. Vugmeister, and H. Daniel Ou-Yang
Physics Department, Lehigh University, Bethlehem, Pennsylvania 18015
(Received 1 March 1993; revised manuscript received 19 August 1993)

We present the results of our experimental and theoretical study of the orientational ordering of rigid-rod-like polymers in the presence of shear flow. Shear-induced birefringence was measured to determine the dependence of the orientational order parameter $S=\langle 3\cos^2\theta-1\rangle/2$ on the shear rate for rod volume fractions below the critical value at which spontaneous ordering at zero shear appears. Experimental results are discussed in terms of an approximate solution of the rotational diffusion equation in the presence of shear flow based on the construction of the effective interaction energy.

PACS number(s): 82.35.+t

I. INTRODUCTION

Recently there has been increasing interest in the problem of the ordering of the rigid-rod particles in flow fields due to its similarity with other problems in nonequilibrium phase transitions [1–5]. It is known that orientational order of concentrated rigid-rod suspensions can occur spontaneously due to preferential packing. Near the critical concentration one also could expect a drastic effect of the flow on the particle alignment, especially at low shear rates where there exists an intriguing cooperative effect between the interparticle interaction (excluded-volume effect) and their interaction with shear flow.

Although the number of theoretical works devoted to this subject continues to increase [6–8], until now no experimental attempts were made to study the effect of the shear flow on the rigid-rod polymeric particles, where contrary to thermotropic liquid crystals [9] the particle density rather than temperature is the driving parameter of the phase transition.

The effect of shear flow on the ordering of the rigid-rod suspension is currently less understood than that for elongational flow. The latter can be described by the potential field that apparently leads to the similarity of the elongational-flow-induced phase transition with the effect of the magnetic or electric field.

For shear flow, there is no simple analytical steady-state solution of kinetic equations that describes the probability distribution of the rod alignment. Because of this, Doi and Edwards [3] (DE) proposed an approach based on the nonequilibrium kinetic equations for the moments of probability distribution. Using a decoupling approximation, they solved these equations and found the steady-state orientational order parameter. However, comparison of the decoupling approximation with the exact steady-state solution for elongational flow clearly shows that its accuracy is limited. In particular, the decoupling approximation cannot reproduce even the mean-field value of the critical concentration of the rods which characterizes their spontaneous ordering in the absence of the flow.

In the present paper we report the results of experimental and theoretical studies of the effect of shear flow on the orientational ordering of monodispersed rigid polytetrafluoroethylene (PTFE) rod suspensions. We measured shear-induced birefringence, which is proportional to the orientational order parameter. The experimental results are compared with the theory based on the approximate solution of the steady-state diffusion equation in the presence of shear flow, which predicts the shear-induced nonequilibrium phase transition from "paranematic" state to nematic state, characterized by different values of orientational order parameters.

II. EXPERIMENT

We use rodlike PTFE rigid particles in aqueous suspension (Ausimont Group, Montedison Specialty Chemicals, NJ) with $L=(0.39\pm0.08)\%$ μm and $b=(0.16\pm0.03)\%$ μm determined by transmission electron microscopy (TEM) of dry samples. The polymer chains in the rod are partially crystalline and aligned along the long axis. The index of refraction is $n_{\parallel}=1.391$ along the long axis and $n_{\perp}=1.368$ along the short axis [10]. The stock suspension has solid content of 32% with approximately 3% surfactant used for colloidal stabilization. We change the concentration by adding deionized water or evaporating excess water to proper concentrations. The highest solid content we are able to prepare is 38%, above which we found the sample less homogeneous and difficult to flow through the cell. We did not attempt to remove the surfactant from the solution.

We use 0.9-cm-wide rectangular quartz cells with 0.02-cm gaps (NSG Precision Glass). The broad sides of the cell are optically polished. The dc shear was generated by a syringe pump (Sage Instruments, Model 351).

The flow cells were placed between two crossed polarizers with an axis at 45° from the direction of the flow (defined as the z direction), as shown in Fig. 1. An Ar-ion laser beam, polarized along the first polarizer and with intensity I_0, is pointing along the dominant velocity gradient of the flow, i.e., the narrow gap of the cell or the x direction. A photodetector (Hamamatsu 1P28A) located at the other side of the second polarizer thus measures the light transmission I_t induced by the birefringence in the sample,

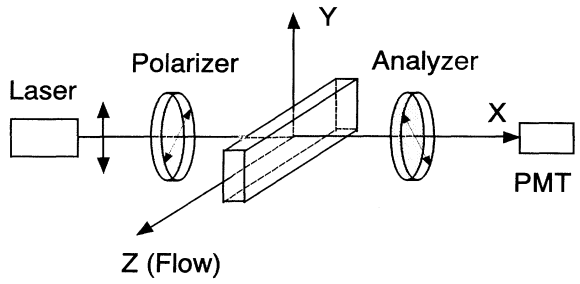

FIG. 1. Optical arrangement of the experiment.

$$I_t = I_0 \sin^2\left[\frac{\Delta\varphi}{2}\right], \tag{1}$$

where the phase shift between the y and z directions of polarization is

$$\Delta\varphi = \frac{2\pi d}{\lambda}\Delta n \tag{2}$$

and λ is the laser wavelength *in vacuo*, d is the cell gap. Experimentally measured birefringence Δn for the geometry of the described experiment can be presented in the form

$$\Delta n = (n_{\parallel} - n_{\perp})(\langle l_z^2\rangle - \langle l_y^2\rangle)C , \tag{3}$$

where l is the unit vector along the long axis of the rod (see Fig. 2), $\langle\ \rangle$ is the thermal average over rod orientations, and C is the rod volume fraction.

Neglecting a small difference between $\langle l_x^2\rangle$ and $\langle l_y^2\rangle$ [11] we can express Eq. (3) in terms of the orientational order parameter $S = (3\langle l_z^2\rangle - 1)/2$,

$$\Delta n = C(n_{\parallel} - n_{\perp})S . \tag{4}$$

The experimental results are presented in Fig. 3, where we plot the dependence of $S = \Delta n/[C(n_{\parallel} - n_{\perp})]$ versus shear rate for different values of the PTFE volume fraction.

One can see that although at higher values of shear rate the order parameter has the tendency to saturate, the absolute values of S differ significantly for different rigid-rod volume fractions. Such a behavior clearly shows that the interaction between rods causes a cooperative effect that promotes their orientational order. In what follows we consider this cooperative effect in more detail.

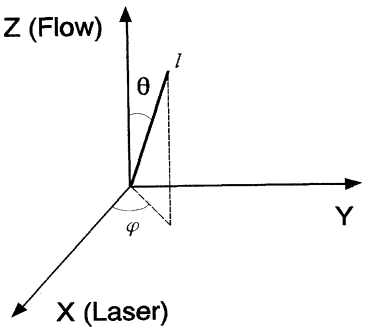

FIG. 2. A rigid rod in a shear flow field.

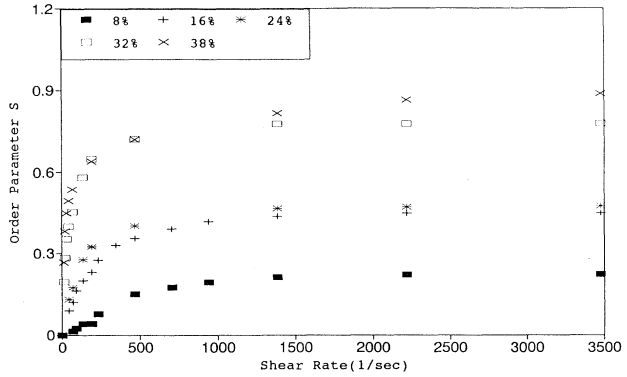

FIG. 3. Measured orientational order parameter S vs shear rate for different rigid-rod volume fractions.

III. THEORY

To consider the effect of shear flow on the rod alignment we start from the simplest model of long and thin rods in a velocity profile with constant velocity gradient

$$k = k_{zx} = \frac{\partial V_z}{\partial x} . \tag{5}$$

Due to symmetry, the orientational order parameter

$$S = S_{zz} = \tfrac{1}{2}\int\int (3l_z^2 - 1)\psi(\theta,\varphi)\sin\theta\, d\theta\, d\varphi \tag{6}$$

depends only on $|k|$, therefore only positive values of k need to be considered. The function $\psi(\theta,\varphi)$ is the orientational probability distribution of the rod in spherical coordinates (with polar axis z, polar angle θ, and azimuthal angle φ). If a rod follows a macroscopic velocity gradient, its angular velocity ω is equal to [3]

$$\boldsymbol{\omega} = \boldsymbol{l}\times(\hat{\mathbf{k}}\cdot\boldsymbol{l}) , \tag{7}$$

where $\hat{\mathbf{k}}$ is the velocity gradient tensor. For the geometry of the flow given above, Eq. (7) can be reduced to the form

$$\omega_\theta = k\sin^2\theta\cos\varphi, \quad \omega_\varphi = 0 , \tag{8}$$

where $\omega_\theta = d\theta/dt$, $\omega_\varphi = d\varphi/dt$.

Condition $\omega_\varphi = 0$ means that flow does not change the orientation of the rods in the φ direction.

A. Dilute solutions

For dilute solutions, neglecting the interaction between rods, we can write the following rotational diffusion equation for $\Psi(\theta,\varphi)$,

$$\frac{\partial\Psi}{\partial t} = \frac{1}{\sin\theta}\frac{\partial}{\partial\theta}\sin\theta\left[D\frac{\partial\Psi}{\partial\theta} - \omega_\theta\Psi\right] + \frac{D}{\sin^2\theta}\frac{\partial^2\Psi}{\partial\varphi^2} . \tag{9}$$

Let us consider the steady-state solution of this equation. In the case of shear flow ω_θ depends on φ as well as on θ according to Eq. (8). In this case, there is no simple analytical steady-state solution of Eq. (9).

To simplify Eq. (9) we notice at first that, for the purpose of calculating the order parameter S, it is sufficient to know only the probability distribution of the polar angle of the rods

$$\Phi(\theta)=\int d\varphi\,\Psi(\varphi,\theta)\ . \tag{10}$$

By integrating Eq. (9) over φ, the second term on the right side of Eq. (9) drops out, and we obtain

$$\frac{\partial\Phi}{\partial t}=\frac{1}{\sin\theta}\frac{\partial}{\partial\theta}\sin\theta\left[D\frac{\partial\Phi}{\partial\theta}-\bar{\omega}_\theta\Phi\right]\ , \tag{11}$$

where we used a decoupling approximation

$$\Psi(\theta,\varphi)=\Phi(\theta)\chi(\varphi)\ , \tag{12}$$

leading to

$$\bar{\omega}_\theta=k\sin^2\theta\int d\varphi\,\chi(\varphi)\cos\varphi=k\sin^2\theta\,\overline{\cos\varphi}\ . \tag{13}$$

The normalized steady-state solution of Eq. (11), according to (13), has the form

$$\Phi(\theta)=\frac{\exp[-U(\theta)/D]}{\int_0^\pi d\theta\sin\theta\exp[-U(\theta)/D]}\ , \tag{14}$$

with the effective potential

$$U(\theta)=-\frac{k}{2}\overline{\cos\varphi}(\theta-\tfrac{1}{2}\sin2\theta)\ . \tag{15}$$

It should be mentioned that a steady-state solution Eq. (14) exists only if we restrict ourselves by the region $0<\theta<\pi$. There is no steady-state solution of Eq. (11) in the region $-\infty<\theta<\infty$, because $U(\theta)$ has no absolute minimum. Because of this property of $U(\theta)$ there is a rotation of the rods in the flow. But in order to find the order parameters we should calculate the average value of l_z^2 which is a periodic function with respect to θ. For averaging such periodic functions, it is sufficient to use the region $0<\theta<\pi$ where a steady-state solution of Eq. (14) exists.

To estimate the unknown parameters $\overline{\cos\varphi}$ we compare the value of the order parameters given by Eqs. (6), (12), and (14) with that determined by DE using a different approximation. One can expect [3] that at higher reduced shear rates

$$\xi\equiv\frac{k}{D}\gg1 \tag{16}$$

the DE approximation is close to exact. In Ref. [3], it was found that

$$\xi^2(1-S_{\rm DE})^3=54S_{\rm DE}\ , \tag{17}$$

which gives, at $\xi\gg1$,

$$S_{\rm DE}\to1-3\frac{2^{1/3}}{\xi^{2/3}}\ . \tag{18}$$

From (6), (12), and (14) at $\xi\gg1$, we have (taking the limit $\theta\to0$ while integrating)

$$S\to1-\frac{\Gamma(\frac{4}{3})}{2\Gamma(\frac{2}{3})}\frac{3^{5/3}}{\overline{\cos\varphi}^{2/3}}\frac{1}{\xi^{2/3}}\ , \tag{19}$$

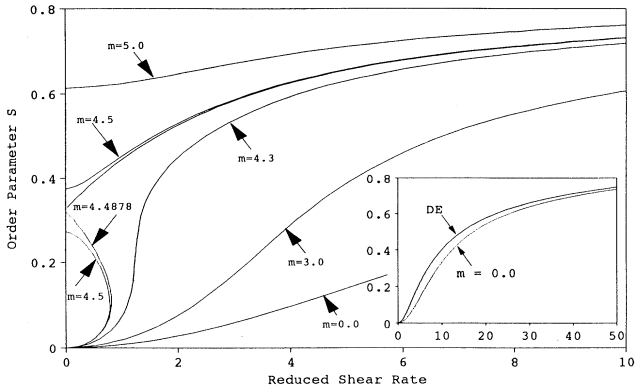

FIG. 4. The theoretical values of S vs reduced shear rate obtained from Eq. (22) for various parameters m.

where $\Gamma(x)$ is a gamma function. Comparing (19) with (18) gives

$$\overline{\cos\varphi}=0.4\ . \tag{20}$$

This value of $\overline{\cos\varphi}$ is not very different from the value of $\overline{\cos\varphi}$ for an isotropic distribution of the rod orientation in the x-y plane. In the inset of Fig. 4, we present the values of $S(\xi)$ obtained from (6), (12), and (14) with $\overline{\cos\varphi}=0.4$ and compare them with $S_{\rm DE}(\xi)$ [Eq. (18)]. One can see that our approximation (16) is in reasonable agreement with the DE approximation. The maximum ratio between two curves has a value of $(S_{\rm DE}/S)\sim2$ at $\xi\to0$ [$S\to\xi^2$ at $\xi\to0$ as follows from the explicit form of Eqs. (6) and (14)].

Although we do not know the exact values of S in the case of shear flow, the data presented in Fig. 4 have the tendency to be less than $S_{\rm DE}$ values. We note that the exact values of S for elongational flow are less than corresponding $S_{\rm DE}$ values [3].

So we can say that Eq. (14) is a reasonable approximation for the probability distribution $\Phi(\theta)$ of orientation of rigid rods in shear flow in dilute limits and it can be used for analyses of more complicated phenomena in concentrated solutions.

B. Effect of rod-rod interaction

To take into account the effect of rod-rod interaction we will use the mean-field approximation for excluded volume potential in the form [7]

$$U_{\rm ex}=-\tfrac{1}{6}mk_BT\sum_\alpha(3l_\alpha^2-1)S_{\alpha\alpha}\equiv-\tfrac{1}{2}mk_BT(3l_z^2-1)S\ . \tag{21}$$

m is the parameter proportional to $nV_{\rm ex}$, where n is the number density of the particle and $V_{\rm ex}$ is the excluded volume.

According to (21) and (14) the self-consistent mean field equation for order parameter S in the presence of shear flow is given by

$$S=\frac{\frac{1}{2}\int_0^{\pi}d\theta\sin\theta\exp[-0.2\xi(\theta-\frac{1}{2}\sin2\theta)+\frac{3}{2}mS\cos^2\theta](3\cos^2\theta-1)}{\int_0^{\pi}d\theta\sin\theta\exp[-0.2\xi(\theta-\frac{1}{2}\sin2\theta)+\frac{3}{2}mS\cos^2\theta]}\ . \tag{22}$$

The numerical solution of Eq. (22) is presented in Fig. 4 in terms of the phase diagram in the (S,ξ) plane. Dashed lines indicate the unstable solutions for which $\partial S/\partial\xi<0$.

One can see that shear flow induces a nonequilibrium first-order phase transition from "paranematic" phase, where $S\ll1$, to nematic phase (in the region where two stable solutions for S coexist) in a manner quite similar to the effect of elongational flow [7]. The important difference, however, is that the two stable regions of S in Fig. 4 extends to much higher values of reduced shear rate ($\xi\sim1$) compared with the rate of deformations for elongation flow ($\xi\sim0.05$) [7]. Such a difference can be explained by the fact that for small values of ξ we have $S\approx\xi^2/100$ for shear flow, and $S\simeq\xi/15$ for elongation flow in dilute regions. Because of this the same orientational effect can be achieved for much smaller values of the rate of elongational deformation compared to the shear rate.

At $\xi=0$, the solution of Eq. (22) gives the value $m^*=5$ as a limit of stability of the isotropic phase, while the phase transition appears at a lower concentration $m_c\approx4.49$. These values cannot be obtained by the decoupling approximation of DE (see also Ref. [7]). The latter gives the value $m^*=3$. The DE approach also has another restriction $S\ll1$ because it deals only with the first three terms of the expansion of the Landau free energy in a power series with respect to S whereas Eq. (22) contains infinite series in S.

IV. DISCUSSION

In the preceding section we have developed a simple approach, which reproduces the main features of the experiment presented in Sec. II, namely, a sharp increase in the orientational order parameter with a shear flow, if the concentration of the rods is slightly below its critical value corresponding to zero-shear isotropic-nematic phase transition.

A question arises, however, as to what extent a quantitative agreement can be achieved between the theory and the experiment, and why there is no clear evidence in the experiment that shear flow indeed can induce nonequilibrium orientational phase transition from a paranematic ($S\ll1$) to a nematic ($S\geq0.5$) state, as it follows from the theory.

In answer to these questions we should notice, first of all, that according to Fig. 4 the bistable region where shear-induced transition does exist is extremely narrow ($4.49>m>4.4$). This means that to observe a phase transition one should be able to change the rod volume fraction by no more than 2%. This makes it difficult to check the predicted transition experimentally.

Second, for quantitative comparison of the theory with the experiment we should take into account that in Sec. III only a case of constant velocity gradient was considered, while a parabolic velocity profile is obviously more adequate for the experimental situation. A parabolic velocity profile results in the distribution of velocity gradients between $k=0$ and k_m with average shear rate $\bar{k}=k_m/2$. In order to include such a distribution in our consideration we should compare with experiment the average value of the order parameter

$$S(\bar{k},D)=\frac{\int_0^{2\bar{k}/D}S(\xi)d\xi}{2\bar{k}/D}\ . \tag{23}$$

Such a comparison is presented in Fig. 5, where the following fitting procedure was used. Curve 1, corresponding to $c=38\%$, was calculated using two fitting parameters m and D. The best fit corresponds to $m_1\approx4.47$, $D_1\approx17\ \text{sec}^{-1}$. The values of parameters m_i for curves 2–4 were calculated using the obvious scaling relation $m_i=m_1C_i/C_1$ and rotational diffusion coefficient D as the only fitting parameter. One can see from Fig. 5 that there is a reasonable agreement between the theory and the experiment for not very large shear rates. The fitted diffusion constants D obtained for different rod concentrations are within a narrow distribution all lower than the value of the estimated free rotational diffusion ($\sim50\ \text{sec}^{-1}$), indicating a hindered rotation in concentrated suspensions.

It is important to note that at the volume fraction of 38% the fitted excluded volume parameter m_1 is very close to the predicted value for the shear-induced nematic transition ($m=4.487$, see Fig. 4) and is only slightly below the spontaneous nematic transition at $m\approx5.0$.

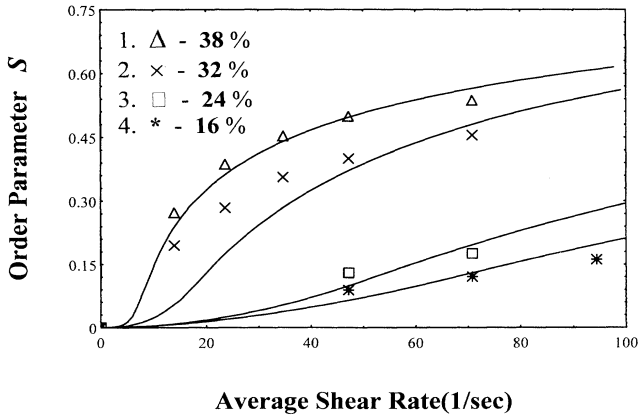

FIG. 5. Comparison between the theory and the experiment based on Eq. (23). Solid lines correspond to the following values of parameters m and D: (1) $m=4.47$, $D=17\ \text{sec}^{-1}$, (2) $m=3.76$, $D=13\ \text{sec}^{-1}$; (3) $m=2.82$, $d=21\ \text{sec}^{-1}$; (4) $m=1.88$, $D=21\ \text{sec}^{-1}$.

For large enough shear rate there are additional factors that make the effect of the shear on orientational ordering more complicated than predicted by the simple theory presented above. (i) As shown by Peterlin and Stuart [12], who considered a limit of very dilute solutions of rod particles, a saturation value of order parameter should depend significantly on the rod aspect ratio, and in general is less than $S=1$, as one can expect from DE and the present approach. (ii) Inertia effects in rod rotation also should be taken into account at high shear rates. In fact, the reduced shear rate can also be referred to as the Peclet number, i.e., a scale to gauge the relative importance of the effect of inertia versus thermal diffusion. Only at low reduced shear rates, when the behavior of the rods in shear flow is governed by diffusion rather than by convection, should our analytical approach using Eq. (9) be valid.

V. CONCLUSION

We have reported experimental observations of the induced birefringence in polymer suspension due to pretransitional orientational ordering of the rigid-rod-like PTFE particles. Experimental results indicate a concentration dependence of the effect of the flow and its drastic enhancement near rod volume fraction $C \approx 38\%$, where there is no spontaneous ordering at zero shear. We attribute this effect to the incipient orientational phase transition from isotropic to nematic phase caused by the excluded volume effect. This experimental observation makes concentrated suspensions of PTFE a potentially interesting candidate for nonlinear optics applications where suspension systems should be just below the critical concentration.

Developed theory predicts also that in addition to spontaneous ordering at zero shear there is a possibility to observe in a very narrow concentration range nonequilibrium phase transition from "paranematic" to nematic phase induced by shear flow. However, in our experiment we have not found unambiguous evidence of the existence of such a phase transition.

ACKNOWLEDGMENTS

The authors thank Peter Olmstead for useful discussions of the results of this paper and Martin Cooksey for assistance with some numerical calculations. We thank the Ausimont Group, Montedison Specialty Chemical for providing PTFE samples for this study. C. Wand and H. D. Ou-Yang thank the Emulsion Polymer Institute, Lehigh, and L. W. Gore and Associates Inc. for partial financial support.

[1] S. Hess, Z. Naturforsch. Teil A **31**, 1507 (1976).
[2] D. Trirumalai, J. Chem. Phys. **84**, 5869 (1986).
[3] M. Doi and S. F. Edwards, *The Theory of Polymer Dynamics* (Clarendon, Oxford, 1986).
[4] S.-Q. Wang and W. Gelbart, J. Chem. Phys. **90**, 597 (1989).
[5] S. D. Lee, J. Chem. Phys. **86**, 6567 (1987).
[6] P. D. Olmsted and P. M. Goldbart, Phys. Rev. A **41**, 4578 (1990).
[7] H. See, M. Doi, and R. Larson, J. Chem. Phys. **92**, 792 (1990).
[8] P. D. Olmsted and P. Goldbart, Mol. Cryst. Liq. Cryst. **198**, 265 (1991).
[9] G. Vertogen and W. H. de Jeu, *Thermotropic Liquid Crystals* (Springer-Verlag, Berlin, 1988).
[10] R. Pizzoferrato, M. Marinelli, U. Zammit, F. Scudieri, and S. Matellucci, Opt. Commun. **68**, 231 (1988).
[11] As a justification of such an approximation, we can refer to the well-known DE decoupling procedure which gives $\langle I_x^2 \rangle = \langle I_y^2 \rangle$.
[12] A. Peterlin and H. A. Stuart, Z. Phys. **112**, 129 (1939); or the review by H. G. Jerrad, Chem. Rev. **59**, 345 (1959).